Title
Predicting Characteristics of the Water Cycle From Scaling Relationships

Journal
Water Resources Research, 57(9)

ISSN
0043-1397

Authors
Hunt, AG
Faybishenko, B
Ghanbarian, B

Publication Date
2021-09-01

DOI
10.1029/2021wr030808

Peer reviewed

Predicting Characteristics of the Water Cycle from Scaling Relationships

A. G. Hunt[1]

B. Faybishenko[2]

B. Ghanbarian[3]

[1] Department of Earth & Environmental Sciences, Wright State University, Dayton, OH 45435

[2] Energy Geosciences Division, Lawrence Berkeley National Laboratory, University of California, 1 Cyclotron Rd., Berkeley, CA, 94720

[3] Porous Media Research Lab, Department of Geology, Kansas State University, Manhattan, KS 66506

Abstract

Over multi-decadal time scales, assuming that changes in subsurface water storage are negligible, the continental precipitative water flux, P, can be divided into two principal components, Q (run-off, including soil infiltration and groundwater recharge) and ET (evapotranspiration). Taking into account a broadly applied Budyko's phenomenology to describe the relationship of ET/P as a function of PET/P, where PET is the potential evapotranspiration, we propose a theoretical framework for predicting characteristics of the water cycle from scaling relationships. In this framework, the ecosystem net primary productivity is expressed in terms of soil formation and vegetation growth, which is mathematically optimized with respect to the water partitioning, generating directly the value ET/P. The mathematical optimization is based on the general ecological principle that dominant ecosystems tend to be those that, for any given conditions, maximize conversion of atmospheric carbon to biomass. It shown that the application the results of mathematical optimization to water-limited ecosystems is

possible by applying the optimization only to a vegetation covered portion of the surface. For energy limited ecosystems, the optimization can be applied only to a portion of the precipitation equal to PET, assuming that the remaining P simply runs off. We use theoretical and actual values of plant root fractal dimensionalities, d_f, to predict ranges of ET/P as a function of PET/P for $0 \leq PET/P \leq 1$ and compare with annual and multi-decadal means of ET/P. By comparing the developed approach with a large amount of data collected from the literature, we demonstrate its successful applications to both water- and energy-limited systems.

1. Introduction

Budyko style equations are commonly used to represent a long-term average of a relationship between the principal hydrologic fluxes, evapotranspiration, run-off and precipitation, on the Earth's terrestrial surface (Schreiber, 1904; Oldekop, 1911; Budyko, 1958; Pike, 1964). Precipitating water, *P*, when it reaches the ground, may partition into several parts - some evaporates directly to the atmosphere, some may run off along the surface, and some penetrates the surface. What enters the soil may be used by plants (transpiration), or reach deeper into the subsurface, where it may replenish oversubscribed aquifers or re-emerge in rivers or springs. Understanding this apportionment is a long-recognized need in the hydrologic sciences (Budyko; 1958, 1974; Manabe, 1969; Lvovitch, 1977; Eagleson, 1978ab; Eagleson and Tellers, 1982; Milly, 1994; Rodriguez-Iturbe et al. 1999; Oki and Kanae, 2006). With sufficiently long period averaging Budyko (1958) and Gentine et al. (2012) argue that changes in storage both in the vadose zone and in the deeper subsurface can be neglected. Then, hydrologic fluxes can effectively be divided into two principal paths, what runs off in streams, *Q*, and what returns to the atmosphere, evapotranspiration, or ET. ET accounts simultaneously for both evaporation and plant transpiration. The Budyko framework represents the fraction of P lost through ET as a function of the ratio of solar irradiance, expressed in terms of potential evapotranspiration,

PET, to P. While knowledge of the total fluxes, P, Q, and ET, are, in general sufficient to describe the global water balance, when the focus of the water balance is at the scale of an individual drainage basin, the ability for water to move between drainage basins in the subsurface adds a level of complexity. The data we have accessed (Gentine et al., 2012) is believed to have been adequately screened to eliminate this possibility, though new research may challenge this assumption (Liu et al., 2020). Chen et al. (2020) discuss a wide range of factors that may confound the determination of simple relationships between P, Q, and ET.

Since the Budyko function accurately describes the trend in ET/P with PET/P, but does not generate any variability in ET/P at a particular PET/P, parametric alternatives to Budyko's function have been developed in the last half century (Fu, 1981; Choudhury, 1999; Zhang et al., 2004; 2008). The question of what drives the variability in ET is, by no means, resolved. Gentine et al. (2012) suggest that the variability tends to disappear as averages are made sufficiently long and that the remaining variability is primarily a result of experimental uncertainty. Since, in our model, the fundamental parameter that arises is a description of the root mass - root lateral spread relationship (a mass fractal dimensionality), our perspective is that the data scatter is reflecting variability in a fundamental property of the ecosystem.

Globally, ET is typically found to be between 0.61 of P (Dai and Trenberth, 2002; Dai et al., 2009) and 0.66 P (Budyko, 1958), and transpiration is about 70% of that (Schlesinger and Jasechko, 2014). This means that, on average, plants tend to use a little less than half of the water available to the land (Schlesinger and Jasechko, 2014). When one accounts separately for the fluxes not penetrating the soil, direct evaporation (e.g., Wang et al., 2007) and overland flow (Jasechko, 2019), the plants still take about 2/3 of the remainder for transpiration (Hunt et al., 2020a). Our purpose is to develop the necessary basis to understand the Budyko framework. Thus, we wish to address the dependence of ET on the ratio PET/P ≡ AI, where PET is known

as the potential evapotranspiration, as well as to predict the variability of ET at a particular value of AI. PET is a variable whose significance was first recognized by Oldekop (1911). If PET/P, called the aridity index (AI), is greater than 1, an ecosystem, or drainage basin, is said to be water-limited; when AI < 1, it is said to be energy-limited.

The fundamental hypothesis (Hunt et al., 2020b) is that the optimization of the ecosystem net primary productivity (NPP) with respect to the partitioning of P into Q and ET forms the basis for predicting ET. Such a basis is distinct from other optimization schemes, which do not relate directly to the hydrologic fluxes (Eagleson and Tellers, 1982; Guswa, 2008; 2010; Milne and Gupta, 2017). However, in order to use a flux-based hypothesis, it is necessary first to be able to predict NPP(Q,ET). This function is built on scaling equations that were predicted to generate soil production and vegetation growth rates (Hunt, 2017), and were, themselves proposed to address more immediate goals, rather than to generate an analytical result for ET in terms of the Budyko variables. In that context, however, it was possible then to use a framework that had already been tested in its individual parts and demonstrated as predictive (Hunt, 2017a; Egli et al., 2018; Hunt et al., 2020c)

The optimization of NPP(Q,ET) was formulated first without taking into account either water or energy limitations (Hunt, 2021). A numerical result for ET/P was obtained whose value, α, depended importantly on root fractal dimensionality, d_f. In systems that were neither energy- nor water-limited, in the limit $d_f \rightarrow 3$, roots take all the water that enters the subsurface and ET → P (α = 1). Extension to water limitations was addressed using a hypothesis that vegetation density is equal to P/PET, and that the optimization applies to that fraction of the area covered by vegetation, with perfect evaporation on the remaining surface (Hunt, 2021; Hunt et al. 2020ab). Extension of the optimization procedure to energy limitations has not previously been addressed, though the known upper bound on ET (= PET) was applied (Hunt

et al. 2020ab). For energy-limited systems, we apply here the optimization procedure only to that fraction of the precipitation that does not exceed PET. Thus, P – PET simply runs off, unaccounted for by our optimization. Applying the optimization procedure to the plant accessible water yields ET = α PET. Here also, the Budyko limit of ET = PET is recovered when $d_f = 3$ and $\alpha = 1$. Applying such related, but not identical calculations, to the AI < 1 and AI > 1 regimes separately carries with it a risk that the approximations do not match at AI = 1. In fact, our derived phenomenology is continuous across AI = 1, but its slope as a function of AI is continuous at AI = 1 only for the single value of $\alpha = 0.5$.

Given a theoretical prediction for the entire range of AI values, we address some basic assessment strategies. The main objective of this study is to try to determine whether experimental results distinguish between the present result and traditional as well as newer formulations. Thus, we begin by showing a comparison with an existing phenomenology (Choudhury, 1999), including identifying approximate relationships between ranges of parameter values. The purpose of this comparison is two-fold: we wish to assess the similarities and contrasts of our predicted form of ET/P as a function of PET/P with existing phenomenologies, while we also wish to check whether there is a correlation between (significant values of) the parameters from the various functions. Then, we wish to determine whether predicted and or observed values of root fractal dimensionality yield a dependence of ET/P on PET/P in accord with data or their summaries. We check first whether the mathematical limits of the Budyko theory correspond to physical limits on root behavior. Then, we check whether there is any relevance of predicted values of root fractal dimensionality based on dimensional constraints to actual data trends. Finally, we use statistical estimates of reasonable limits of the root fractal dimensionality, d_f, from experiments carried out on grasses (Levang-Brilz and Biondini, 2002) to determine whether these values sweep out experimental ranges (Gentine et al. 2012) of ET(P) as a function of

aridity index. In this, we investigate discrepancies between our predictions and observations at high values of the aridity index, in order to try to understand the cause of such a discrepancy. In the process, we are able to draw conclusions about the efficiency of the water use of forests under distinct climates with the same AI values, as well as about the necessity to extend the formulation to drainages for which both conditions of water- and energy-limitations can be relevant, but at different times of the year. We also suggest that neglect of drawdown of aquifers as well as such fluxes as fog and dew degrade performance of Budyko type models generally at high aridity index, including our own predictions.

2. Theoretical Background

The percolation theoretic approach was successfully applied to develop a fundamental framework for the soil depth (Egli et al., 2018; Yu and Hunt, 2017ab; Yu et al., 2019) and vegetation productivity (Hunt, 2017; Hunt et al., 2020b). The basis for these flux-based calculations is found in the tendency for water flow in porous media to be dominated by connected paths of optimal impedance (Hunt and Sahimi, 2017). Considerable emphasis has been placed on locating or defining such paths in soils and regolith (Bundt et al., 2001); mostly the cause has been sought in such intrusive biological phenomena as decaying plant root structures, and invertebrate activities (Flury and Flühler, 1994; Stagnitti et al., 1995). The statistical variability of the connection of such paths seems beyond enumeration. Within the context of percolation theory (Hunt and Manzoni, 2015), however, the hypothesis is formulated that all such “preferential flow” paths can be described with a network of local resistances at the pore scale. This network is then fully characterized by the probability density function for the local resistance values and any correlation structure in the positions of the resistances. Now, the question is, what advantages does such a conceptual picture bring with it? A key problem in hydrogeosciences since the late 1980’s is the scaling of properties with distance as controlled by the connectivity and tortuosity of

dominant flow paths in disordered media (e.g., National Research Council, 1996). A network basis allows the investigator to tap into a body of literature based on percolation theory (e.g., Sheppard et al. 1999; Lee et al. 1999), with which to ground predictions of the spatio-temporal behavior of fluid flow and solute transport, which underlie such phenomena as chemical weathering and soil formation (Maher, 2010; Yu and Hunt, 2018).

While our focus has been on the simplest predictions of hydrologic variables that can be made using percolation theory, a background literature also exists for cases when simple is not sufficient (Sahimi, 1994), for example, when long-range correlations between the local resistance values exist. Our perspective has been to use the uncorrelated framework to generate universal scaling predictions and seek for the variability in the soil medium in terms of the variability of the scale factors, rather than in the scaling functions, as will be clarified.

Sahimi (1994) argued that, in media that are sufficiently disordered that water flow is dominated by percolation's critical paths, solute transport will obey the percolation scaling relationship expressed by Lee et al. (1999) in simple terms

$$t \quad x^{D_b} \tag{1}$$

Here, t is the time, x is the transport distance, and D_b is the fractal dimensionality of the percolation backbone, which can take on several different values. However, in the context of soil formation, our focus, D_b is associated with downward water fluxes, and for three-dimensional connectivity D_b should be either 1.87, for saturated conditions, or 1.86, for wetting conditions (Sheppard et al. 1999), a distinction which is negligible. The fact, that $D_b > 1$ implies retardation in the solute transport as well as a slowing of reaction rates. The slowing is a result of the topological complexity of those preferred flow paths near the percolation threshold that define the water flow rate, and also have orders of magnitude lower

cumulative resistance than non-preferred paths. For dimensional consistency, rewrite Eq. (1) as

$$x = x_0 \left(\frac{t}{t_0} \right)^{\frac{1}{D_b}} \quad (2)$$

In Eq. (2), x_0 is the fundamental spatial scaling factor, as a network node separation, or the median particle size, d_{50}, and t_0 is the ratio of d_{50} to the mean annual vertical flux at the pore scale, which is (P – ET)/ϕ, where ϕ is the porosity (Yu and Hunt, 2017). When erosion is negligible, Eq. (1) gives the soil layer depth (Hunt, 2017). In the case of surface reactions in porous media, such as weathering, solute transport is limiting, and the product of the solute velocity, dx/dt, and the molar density of the weathering products gives the weathering rate. Provided chemical weathering limits soil formation (Yu and Hunt, 2017), dx/dt also generates the soil production rate. If the soil production and denudation rates, D, are the same, the steady state soil depth, d, is given by (Yu and Hunt, 2017a);

$$d = d_{50} \left(\frac{P - ET}{1.87 \phi D} \right)^{\frac{1}{D_b - 1}} \quad (3)$$

The results of Eqs. (2) and (3) for d have been verified for 10 yr < t < 10^8 yr (Yu and Hunt, 2017b), 1 m/10^6 yr < D < 1000 m/10^6 yr (Yu and Hunt, 2017a) and 2mm/yr < P < 10 m/yr (Hunt and Ghanbarian, 2016), as well as for slope angles from 0 to 45° (input to D) (Yu et al. 2019), while, for typical values of all parameters, Eq. (3) gives the typical soil depth of about 1m. Most important for the water balance is that $d \approx$ (P-ET)$^{1.15}$ in steady-state (using D_b = 1.87). Results obtained independently by Khormali et al. (2012) demonstrate a proportionality of (loess-derived) soil depth to P along a climate gradient.

The vegetation growth framework ties the percolation optimal paths tortuosity (Porto et al. 1997) to root extension paths. Growth along optimal paths optimizes simultaneously access to water and nutrients (Bundt et al.

2001), while minimizing metabolic cost (Hunt and Manzoni, 2015). The essential distinction between root growth and solute transport is that plant roots are directed networks and hierarchical, avoiding the closed loops followed by solute transport. Exponents that describe root tortuosity are consequently much nearer 1 (meaning less tortuous paths) than are the exponents describing slowing of solute transport. The tortuosity of the optimal paths controls their complex development. The optimal paths exponent has a dependence on dimensionality. The choice of D_{opt} = 1.21, appropriate for consideration of the 2D flow domain, is based on an extensive comparison with the data for the temporal evolution of a root lateral spread (RLS) (Hunt, 2017). The scaling equation for RLS is then based on the assumption that mean root tip extension rates are scale-invariant (like the water flow rate in Eq. 2), making the result analogous to Eq. (2), but with a different non-linear power. The consequence of the non-linear power is that the reference parameters develop a scale dependence. In the particular case of root growth, the result is most transparent when upscaled to the growing season time, t_g and length, T_g, scales, with T_g being the transpiration depth (Hunt et al., 2017).

$$RLS = T_g\left(\frac{t}{t_g}\right)^{\frac{1}{D_{opt}}} = T_g\left(\frac{t}{t_g}\right)^{0.83} \quad (4)$$

Further verification for this result was given in Hunt et al. (2020c). Note that, for $t = t_g$, the RLS has increased in length by T_g. If the root mass is characterized by a mass fractal dimensionality, d_f, then the added mass at $t = t_g$ can be expressed as, $m = \left[RLS\left(t_g\right)\right]^{d_f}$, or more simply, as,

$$m = T_g^{d_f} \quad (5)$$

Taking into account that the transpiration is the major part of ET, and the root mass is a critically important input to the NPP, it is possible to rewrite Eq. (5) approximately as (Hunt, 2017)

$$NPP \approx ET^{d_f} \quad (6)$$

Since the spatio-temporal scaling of the RLS was found to be governed by 2D exponents (Hunt and Manzoni, 2015; Hunt, 2017), the consistent choice for d_f was considered to be the 2D percolation value of 1.9 (Hunt, 2017). But, for the 2D case, Eq. (6) only accounts for the horizontal component of the root development affecting the NPP, and must also be multiplied by the vertical extent, d,. Thus, root mass may be mostly confined to 2D, but will still be proportional to the depth of the root mass, which is very nearly the solum depth (e.g., Gentine et al. 2012; Fan et al. 2017, Lynch, 1995), Eq. (3). Thus,

$$NPP \approx ET^{1.9}(P-ET)^{1.15} \quad (7)$$

Here 1.15 was substituted for 1/(1.87 – 1). The maximum NPP may be found by setting d(NPP)/d(ET) = 0 and solving for ET. Performing this optimization on Eq. (7) with respect to ET yields

$$ET=[1.9/(1.9+1.15)]P=0.623P \quad (8)$$

The value, 0.623P, is comparable to the global average ET, a surface area weighted average over all climate regimes, that is given as 0.634 P (Williams et al. 2012). Related, but slightly different values for the global ET, are cited in Hunt et al. (2020a). On global scales, root systems are indeed shallow, while global ET, constrained by PET, is also equal to P.

Hunt et al. (2020a) then address effects on the prediction of ET due to such factors as interception (Wang et al. 2007) and the partitioning between surface and subsurface run-off (Jasechko, 2019).

It was proposed (Hunt et al. 2020ab; Hunt, 2021), that when root systems are deeper due to critical requirements for water (Fan et al. 2017), the appropriate value of the optimization constant is found for the 3D percolation value of d_f, 2.5. Consider how Eq. (7) and Eq. (8) would change if the relevant root fractal dimensionality were d_f = 2.5. For consistency in units, the power (P-ET) from the soil depth factor in Eq. (7) would have to be replaced with $(P-ET)^{(3-d_f)1.15}$. Optimization of $ET^{2.5}\left[(P-ET)^{1.15}\right]^{0.5}$ leads to ET = 0.813P. For d_f =

3, Eq. (7) would then yield $NPP \approx ET^3 \left(P-ET\right)^{\left|3-3\right|1.15}=ET^3$. In this limit, our optimization procedure yields ET = P, as there is no factor to reduce productivity even if the roots take all the water that arrives in the soil. Thus, there is no local maximum of NPP within the range of allowed values of ET. We express this suite of results as ET = α P, where α = α(d_f), and takes on values of 0.465, 0. 623, 0.813, and 1 for d_f = 1, 1.9, 2.5, and 3, respectively.

How does our prediction for ET vary with climate, expressed in terms of the aridity index given as AI = PET/P?

Hunt (2020) suggested that the optimization scheme could apply to vegetation present, even for AI >> 1, but that such vegetation could, at most, occupy the surface area equivalent to a fraction P/PET, while evaporation is 100% from the remaining surface. The result was,

$$\frac{ET}{P}=1-\left(1-\alpha\right)\frac{P}{PET} \tag{9a}$$

$$\frac{Q}{P}=\left(1-\alpha\right)\frac{P}{PET} \tag{9b}$$

where the second equation follows from Q + ET = P. For the case d_f = 3, α = 1, and for all AI > 1, ET/P = 1, the Budyko limit. Otherwise, there is an important distinction with the Budyko function. Budyko phenomenology requires 1-(ET/P) ≈ $(AI)^{-2}$, what we refer to as quadratic asymptotics. Therefore, Eq. (9) and Eq. (10) (linear asymptotics) are distinct from Budyko's phenomenology.

3. Extensions of Theory and Comparison with Existing Phenomenology

Since plant root models in the context of percolation theory can thus extend from 2D to 3D, we hypothesize that practical long-term, steady-state bounds on the water balance components for AI ≥ 1 are provided by the 2D and 3D results given in Eq. (8) and Eq. (10). We wish to estimate corresponding limits in the regime AI ≤ 1.

The simplest theoretical alternative for the energy-limited regime (AI < 1) is to assume that P – PET simply runs off, unaccounted for, and that the optimization applies to the remaining P equal to PET; thus, one has ET = α PET. Then,

$$\frac{ET}{P}=\alpha\frac{PET}{P} \qquad (10a)$$

$$\frac{Q}{P}=1-\alpha\frac{PET}{P} \qquad (10b)$$

If the actual plant (or ecosystem) value of $d_f = 3$, then $\alpha = 1$, and the result ET/P = PET/P is recovered. Thus, for $d_f = 3$, the known limits for ET on the Budyko plot are recovered for all AI. In general, at AI = 1, Eq. (9a) and Eq. (10a) both yield ET/P = α, while Eq. (9b) and Eq. (10b) both yield Q/P = 1- α. Theory thus produces continuous behavior for AI < 1 and AI > 1 for any specific value of α. Two points must be made, however. One is that the derivative of ET/P with respect to AI is not continuous, except for the case α = 0.5. Further, there is no guarantee that any particular trajectory across Budyko space in natural systems will require a consistency of α across the entire range of AI values. As water becomes scarcer with increasing AI, root depths increase (Fan et al., 2017), which we should expect to lead to less anisotropy of the root system and a higher fractal dimensionality. Thus, we may expect a cross-over to higher values of α with increasing AI, although there is no reason to expect that this cross-over will occur at any particular value of AI. Finally, although systems for which PET/P < 1 are classified as energy-limited, if the precipitation arrives in winter and the bulk of the solar irradiance in summer, they may still experience significant water limitations. Therefore, our conceptualization of a rigid distinction between energy- and water-limited systems is oversimplified and might be improved by a composite treatment, allowing separate limitations for distinct fractions of a year. Nevertheless, for those sets of data that we are aware of, experimental

scatter is of sufficient magnitude that this theoretical limitation is not of significance.

For later comparison with experiment in the water-limited regime (AI > 1), Eq. (9) is rewritten as,

$$\frac{ET}{PET}=\left(\frac{P}{PET}\right)\left(1-(1-\alpha)\frac{P}{PET}\right) \qquad (11)$$

Budyko theory has, up until now, mostly inspired multiple mathematical developments, and a limited publications presented new physical, development. For example, Sposito (2017a,b) incorporated into the Budyko's framework the changes in vadose-zone water storage in a manner that is both parsimonious in hypotheses and broad in scope. As pointed out by Budyko (1958), clear limits on ET/P exist in the limits when PET/P approaches zero and infinity. In the former, ET cannot exceed PET; in the latter, P provides a similar upper bound. Mathematical functions are sought that conform to these general results. For parametric functions (which give a continuous range of predictions in terms of a parameter), these results may be obtained exactly from applying a limiting value of that parameter. A range of proposed functions is presented in Table 1. The results are expressed traditionally in terms of $\varphi \equiv PET/P$. Schreiber's and Oldekop's formulations were considered lower and upper bounds for ET/P, while that of Budyko, typically superior *in the mean*, was formulated as the geometric mean of these bounds (Choudhury, 1999). More recent phenomenologies (Fu, 1981; Choudhury, 1999; Zhang et al., 2004; 2008) are most easily conceptualized in terms of a generalization of the Pike phenomenology. Choudhury (1999), for example, replaces Pike's powers 2 and ½ by arbitrary reciprocal fractions n and $1/n$, with $n > 1$. The original Pike phenomenology is scarcely distinguishable from Budyko (Choudhury, 1999); however, Choudhury's (1999) generalization allows it to generate a much wider range of ET values at any specific AI value than that generated by Oldekop's and Schreiber's functions together. A significant, unanswered, question is: how

much variability should be contained within a single, universal, function for ET/P?

Table 1. Various models relating evapotranspiration *ET* to precipitation *P.*

Model	**Reference**
$f(\varphi)=1-\exp(-\varphi)$	Schreiber (1904)
$f(\varphi)=\varphi\tanh(1/\varphi)$	Oldekop (1911)
$f(\varphi)=1/\sqrt{1+1/\varphi^2}$	Pike (1964)
$f(\varphi)=\left[\varphi\tanh(1/\varphi)(1-\exp[-\varphi])\right]^{0.5}$	Budyko (1958, 1974)
$f(\varphi)=1/\left(1+(1/\varphi)^n\right)^{1/n}$	Choudhury (1999)

4. Comparison with other models and experimental data

4.1. Percolation predictions of ET/P

Figure 1 shows a comparison of the results of our physically-based model with one of the parametric models cited above (Choudhury, 1999). Reflecting the physical nature of our model, the Budyko limit on ET is recovered for d_f = 3, in contrast to the Choudhury mathematical model, for which the Budyko limits are recovered in the limit of infinite *n*. Recall in this context that the limiting value of d_f = 3 arises from a (physical) dimensional constraint; the horizontal (RLS) and vertical (depth) dimensions of the root system cannot together account for more than 3 dimensions of root mass. A mathematically less rigorous, but still physically significant bound is represented by d_f = 1, a linear relationship between RLS and BGB.

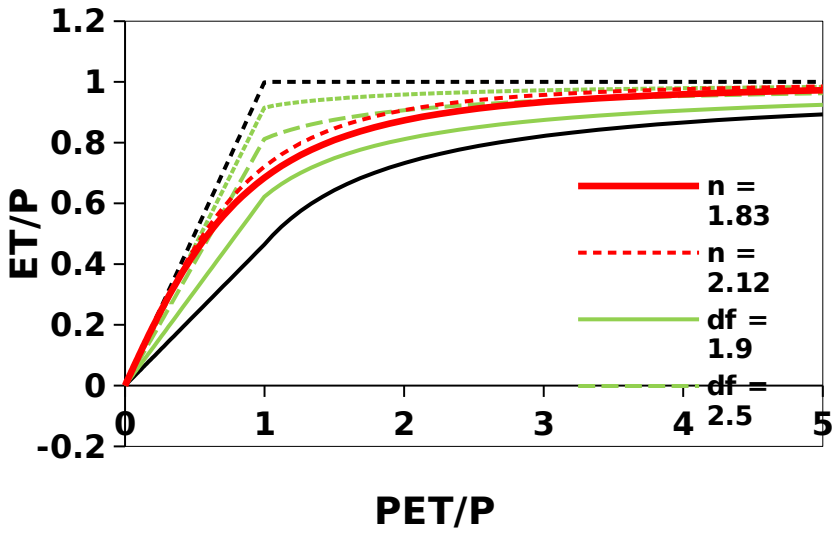

Figure 1. Comparison of the Budyko function derived from the optimization of NPP with respect to ET with the Choudhury (1999) function for various values of *n* for the Choudhury function, and d_f for the percolation function.

Note that, for AI > 2.5, curves generated by percolation theory are essentially indistinguishable from those of the Chowdhury (1999) phenomenology. In the range AI < 1, Chowdhury (1999) curves resemble closely percolation predictions for $3 - d_f << 1$. The percolation theoretical formulation tends to generate a broader range of possible PET/P values than the Choudhury function for any given ET/P when AI < 1. This distinction results from the fact that, in contrast to other Budyko formulations, only for $d_f = 3$ does the percolation formulation predict a slope of 1 in the limit AI → 0; otherwise, it predicts a smaller slope (= α). Applying a relationship similar to that of Choudhury (1999), Zhang et al. (2004) found an average parameter (ω) value of 2.84 for forested catchments with an average ω of 2.55 for grassland. Using analysis of Yang et al. (2008), it is possible to approximate the value of (Choudhury's) n as ω – 0.72, which yields n = 2.12 for forested catchments, n = 1.83 for grasslands. This is the reason these n values are shown. The d_f values shown are 1.9 (2D theory), 2.5 (3D theory),

and 2.78 (one standard deviation above the mean for Grass Group 1 from experiments by Levang-Brilz and Biondini (2002); see section 4 below, for a discussion quantifying variability of d_f).

Also note in Figure 1 that the physical constraints $1 \leq d_f \leq 3$ provide a predicted bound for data which, except in the region AI < 0.5, is in reasonably close agreement with the mathematical formulation of Choudhury for the range $1 \leq n \leq \infty$. Moreover, the percolation prediction for $d_f = 2.5$, the 3D theoretical value for root fractal dimensionality, is in rather close correspondence to Choudhury's model prediction for n = 2.12 (ω = 2.84 in Zhang's model) over the entire range of PET/P, considered valid for forests. A third important result from Figure 1 concerns sensitivity. The distinction between the predictions for $d_f = 1$ and $d_f = 2.1$ is considerably smaller than the corresponding distinction between the predictions for $d_f = 2.1$ and $d_f = 2.9$. This is not surprising, as our limit of $d_f \rightarrow 3$ corresponds to the Choudhury limit of $n \rightarrow \infty$. Thus, sensitivity to input root measurements increases with increasing d_f, a measure of the space-filling ability of the plant roots.

For later context, Figure 2 shows a comparison between the predicted range of ET values from percolation theory and the ca. 18,000 data points from Figure 1a of Gentine et al. (2012).

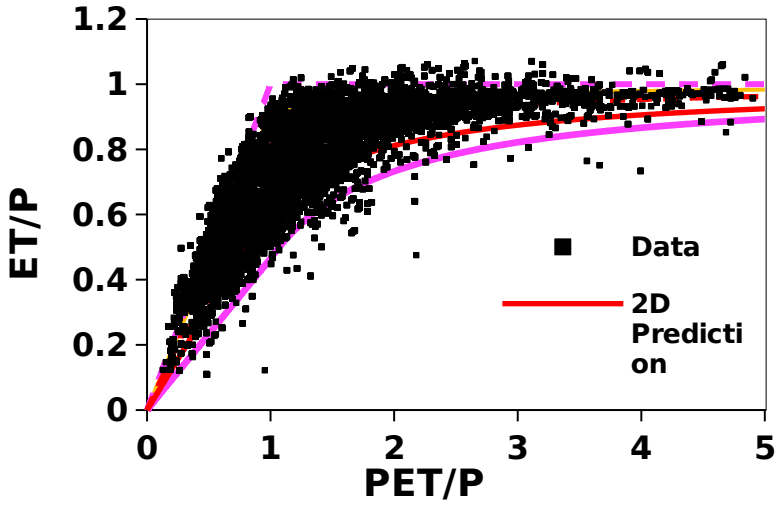

Figure 2. Percolation predictions of ET/P as a function of PET/P. Approximately 18,000 data points shown on the figure were digitized from Figure 1a of Gentine et al. (2012).

The 2D and 3D predictions use the theoretical values from percolation theory for root fractal dimensionality that are characteristic of large clusters near the percolation threshold. $d_f = 3$ is a theoretical maximum (completely space-filling) fractal dimensionality, for which roots can extract all water entering the soil, $d_f = 1$ is a physical minimum that represents a purely linear relationship between below-ground biomass and root lateral spread. $d_f = 2.78$, as will be seen, is an upper bound established by plants growing in pots (Levang-Brilz and Biondini, 2002) that was determined by assuming that plant root fractal dimensionalities are distributed according to a Gaussian distribution. While, on the whole, the theoretical extreme values of d_f (1 and 3) constrain the observed data very well, theory does appear to underestimate observation somewhat at high AI values.

In Figure 2 the ability of the percolation theoretical construction for ET/P as a function of PET/P is tested to see if its theoretical parametric values are in accord with a wide range of data and whether its upper and lower bounds

constrain the large majority of the data. From the figure, it appears as though the predicted values of d_f underestimate ET/P somewhat at higher PET/P values. Much of the remaining text is devoted to this (small) discrepancy. We note, however, that an analogous model underestimation of ET/P is seen at higher values of AI (> 2.1) in the comparison of Budyko theory with experiment in Gentine et al. (2012) Figure 1b.

4.2. Water Balance Data

Since the simplification of the fluxes, as described in the traditional water balance, requires long-term drainage basin averages of Q in order to neglect changes in storage and infer ET as $P - Q$, when our results are compared with data, it can be useful to reference long-term averages. When short-term data is accessed, some effort should be expended to constrain effects of storage changes. This could include random fluctuations from weather-related inputs, as well as systematic influences from climate or land-use changes. We suggest that ET/P ratios may often be overestimated on account of underestimating the denominator, P. Water input to the system from drawdown in storage, if neglected, will also produce a tendency to overestimate the fraction of input water lost to ET.

In addition to the data digitized from Figure 1a of Gentine et al. (2012) and shown in Figure 2, we have also digitized longer-term data, including the data presented in Figure 3 of Duan et al. (2006). These data are not presented in the traditional Budyko form, and we have retained their presentation variables (ET/PET and P/PET = AI^{-1}). These data were obtained for 12 representative drainage basins in conterminous USA (listed in Duan et al. 2006). Gentine et al. (2012) accessed the complete climatological and streamflow data set from MOPEX (431 drainage basins), together with all the necessary codes for generating Budyko datasets, but ultimately confined their study to a subset of 354 basins, for which results could be based on at least 50-year averages. In Figure 1a of Gentine et al. (2012), the yearly ET/P data were plotted against PET/P. In Figure 1b, they presented the 50-year

average data for the same 354 basins that were represented in their Figure 1.

4.3. Root characteristics

We also used data for actual plant root characteristics (extracted from Levang-Brilz and Biondini, 2002) to investigate the implications of the variability actual plant architecture on a Budyko plot of ET/P vs PET/P. Previously (Hunt et al. 2020ab, Hunt, 2021), we had largely taken fractal dimensionality values from individual plant species; here, we attempt to generate representative values and their typical variability. We note that finding characteristic root fractal dimensionalities from a data aggregate over similarly behaving species moves us somewhat closer to finding the effective fractal dimension of an ecosystem, and its spatial variability.

Levang-Brilz and Biondini (2002) grew 55 species of plants common in the Great Plains ecosystem in pots and then extracted them to measure their below-ground biomass (BGB) and root lateral spread (RLS) (and other quantities). The data for RLS as a function of root mass (yielding $1/d_f$) were collected under conditions that minimized both light and water limitations. The species chosen were typical of Great Plains USA ecosystems, for which grasses make up over 90% of the biomass (Barker and Whitman, 1988). The authors noted that, taken in aggregates, the fractal dimensionalities of the roots of the grasses separated into two groups, one of which was characterized by $d_f = 1.79$ and one for which $d_f = 2.65$. These values differ from the predicted d_f values from percolation in 2D (1.9) and 3D (2.5) only by about 6% (Stauffer and Aharony, 1994). The aggregate fractal dimensionality of the forb species was reported to be 2.5, although there was large variability among these species as well.

As the statistics of the grasses of Grass group 1 appear to have the greatest significance to the experimental results, the names and fundamental characteristics of the members of this group are given in a table below. Mid and Late refer to the time in seasonal succession. However, there is no

obvious adaptive distinction between these grasses and those of Grass group 2, which are also distributed among Mid and Late successions as well as C_3 and C_4 types.

Table 2. Species names and results for scaling of RLS with BGB for Grasses group 1 (from Levang-Brilz and Biondini). $s = 1/d_f$ is the exponent in the power law RLS =A BGB^s (with constant parameter, A)

Type	Genus	Species	*s*
Mid C_3	*Agropyron*	*cristatum*	0.007
Mid C_3	*Bromus*	*inermis*	0.496
Mid C_3	*Hordeum*	*jubatum*	0.67
Mid C_4	*Sporobolus*	*cryptondras*	0.443
Late C_3	*Agropyron*	*spicatum*	0.527
Late C_3	*Elymus*	*canadensis*	0.439
Late C_4	*Andropogon*	*gerardii*	0.515
Late C_4	*Calamovilfa*	*longifolia*	0.373
Late C_4	*Panicum*	*virgatum*	0.202
Late C_4	*Schizachyrium*	*scoparium*	0.534
Late C_4	*Sorgastrum*	*nutans*	0.348

We digitized the results of Levang-Brilz' analysis (their Figure 1A) for the relationship between BGB and RLS for the two groups of grasses. The process of digitization introduced a small error: our extracted best fit power (Grass 1) for RLS = A BGB^s is $s = 0.3821$ ($d_f = 2.62$) instead of the value of

0.3767 (d_f = 2.65), obtained by Levang-Brilz and Biondini (2002), though our value for A was the same (0.245). Our result for Grass 2 produced a similar discrepancy, s = 0.5637 (d_f = 1.77) instead of 0.5597 (d_f = 1.79), indicating a small uncertainty in data interpretation.

In order to estimate the uncertainty in d_f, we used first the digitized data (Figure 3ab here) to generate reasonable estimates of maximum and minimum values of s that constrain the data, while using the same value of the prefactor A. Our results were as follows: for Grass 1, s_{max}= 0.465 and s_{min} = 0.30 (d_f = 2.17 and 3.33) with centroid 0.382 and corresponding d_f = 2.62, and for Grass 2 (s_{max} = 0.62 and s_{min} = 0.50), with centroid 0.56 corresponding to d_f = 1.79. We find that roughly 90% of the data points are located within these bounding estimates, an approximate correspondence with a two standard deviation range. It follows that a single standard deviation would cover a range of s values half as wide, yielding upper and lower bounds for the aggregate d_f values of Grass 1 equal to 2.93 and 2.36, respectively.

As an alternate approach, below, we use the data from Table 2 for individual species s values, together with an ansatz that the s values fit a Gaussian distribution to generate a mean (and its standard deviation) for s among the species from Group 1. From these statistics of the power s, we develop an upper and lower bound for the expected values of d_f. The two methods to generate a range of d_f values are not mathematically equivalent, but close correspondence between the two results would generate some confidence in their use.

Using the last column of Table 2, we find for Grass 1, a mean $\acute{s}=¿$0.414 ± 0.054. Using d_f = 1/s yields for a best estimate of d_f = 2.42, which is lower than the value (2.65) determined by Levang-Brilz. The corresponding results for a minimum and maximum d_f for Grass 1 are then 2.13 and 2.78 (instead of 2.36 and 2.93, above). All three values are smaller than our graphical estimate by about 0.2. Given the rapidly increasing sensitivity of ET to d_f as

d_f approaches 3, the uncertainty in d_f has a much larger effect on the estimates of the upper bounds of the expected ET than on the lower bounds. In the comparisons with data, we will use the second method as the standard, since it is unambiguously quantifiable, but note that the first method is a potentially equally valid alternate choice.

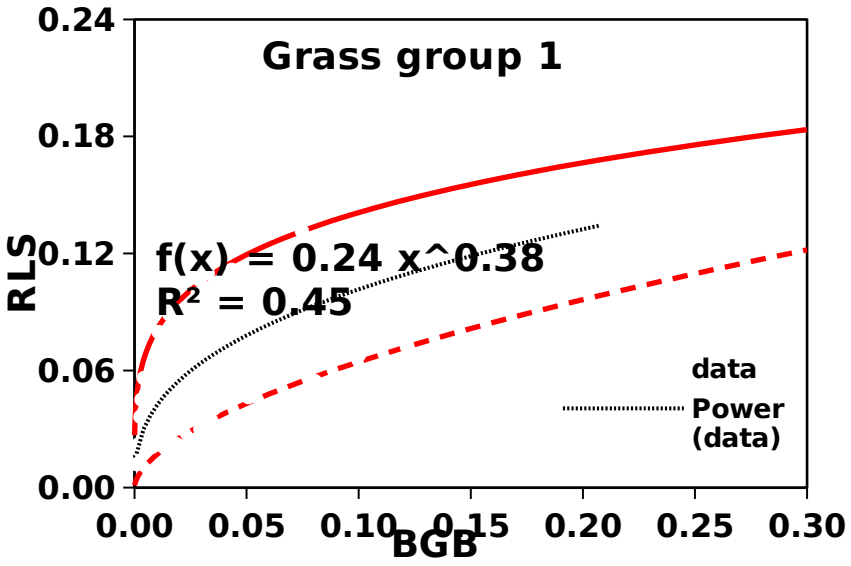

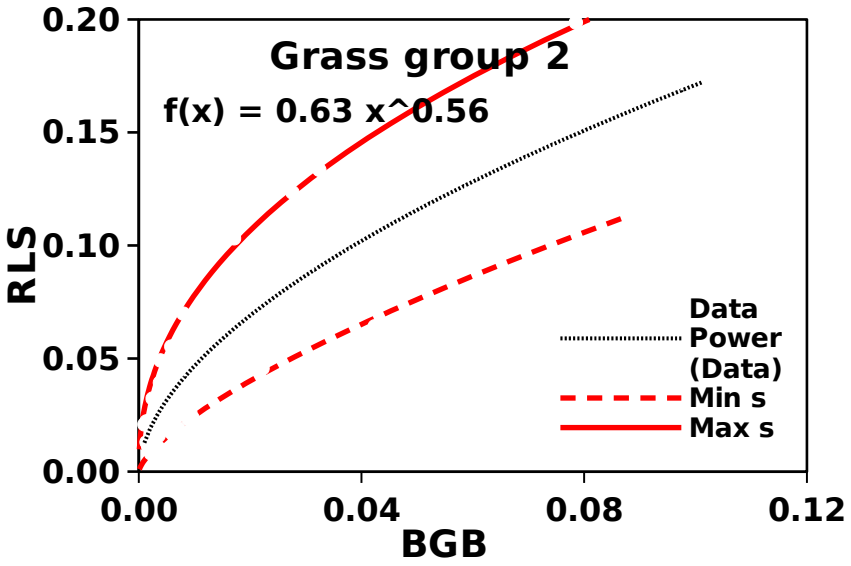

Figure 3. A demonstration of our estimates of the upper and lower bounds of *s* in the relationship between BGB and RLS for the data of Levang Brilz and Biondini (2002). Figure 3a is for grass Group 1, and Figure 3b for grass Group 2, both groups as determined by Levang-Brilz and Biondini (2002).

These bounds on s correspond, respectively to the lower and upper bounds of expected $d_f = 1/s$. About 8/95, or 8%, of the data points lie outside the estimated bounds in Figure 2b, but 24/190, or 13%, in Figure 3a.

4.4. ET Measurement Biases at Large ET or AI

Note that a fundamental objective of the work of Gentine et al. (2012) was to suggest that the explicit form of the Budyko's ET (P) relationship could account for all the long-term average data, if one assumed that the variability in the data were essentially attributable to random experimental error. Thus, in order to generate reasonable uncertainty in prediction, Gentine et al. (2012) applied ±10% adjustment to the original Budyko function, citing Potter et al. (2005) to support this magnitude of uncertainty for meteorological data. However, this approach makes long-term average ET/P values as high as nearly 1.1 for AI = 5, which, in this picture, could only be acceptable as a random error. Analysis of Figure 1b of Gentine et al. (2012) shows that at least 80% of the data for long-term averages *exceed* the Budyko prediction for AI > 2.1. Thus, unless there is a systematic experimental error at high AI, the Budyko function appears also to underestimate ET in this range. Our theoretical perspective attributes significant variability to ET from plant root architecture, but we also cannot argue that ET should exceed the Budyko limit (i.e., ET/P > 1). Since both our new formulation and that of Budyko appear to underestimate ET for large AI, we investigated potential systematic biases that could lead to model overestimation of ET at high AI. For this purpose, we consider two types of bias: 1) diminution in groundwater storage from either climate change effects on, or exploitation of aquifers in agriculture, and 2) underestimation of precipitation at high AI.

Worldwide estimates of groundwater depletion vary significantly and are of interest for their potential contributions to sea level rise (Wada et al. 2017). Pre-2000 estimates vary from 0.075 mm yr^{-1} to 0.3mm yr^{-1} (Wada et al. 2017). More recent studies of the global water budget suggest mean

storage losses as high as 0.71mm yr^{-1} (Wada et al. 2017). The data of Gentine et al. (2012) are exclusively from drainage basins in the USA, and most authors agree that there has been sufficient water demand from agriculture in the USA to deplete water resources significantly. Specific numbers on this vary; Liu et al. (2018) give a yearly mean depletion of almost 4% of P (20 mm yr^{-1}) in the Columbia basin, approximately 0.4% of P (3 mm yr^{-1}) in the Mississippi drainage, and 0.5% of P (7 mm yr^{-1}) in the Pearl River basin, but discuss no other USA river drainages. After (areal) averaging, the best estimate for these three basins is, annually, 0.8% of P storage loss. Their (areal) average AI value is 1.41, but the depletion to storage tends to increase with increasing aridity index, and is largest in the Columbia River basin.

For the second potential confounding input, we consider precipitation measurements. Actual measurement of precipitation is less accurate than often assumed. Rainfall during intense events can, using tipping buckets, be underestimated by more than 30% (Sypka, 2019). Light rainfall, fog, and dew are difficult to capture accurately by any method. Moratiel et al. (2016) state, “If the canopy is wet due to fog, dew, or light rainfall, however, energy contribution to surface evaporation will reduce transpiration and hence soil water losses. When surface evaporation occurs, the ET overestimates the soil water depletion by an amount approximately equal to the surface water evaporation.” Thus, the ratio of ET/P may be overestimated by a fraction similar to the contribution to P of fog or dew. In order to estimate a magnitude of this effect, we conducted a literature survey (Table 2). Daily contributions of fog or dew to P were typically in the tenths of millimeters, annual values measured in centimeters. Such a contribution to P is obviously of greater significance in arid regions, where annual precipitation is typically less than 20 cm, and often less than 10 cm. The mean and standard deviation values of the fractional underestimation, 0.11 ± 0.08, calculated from the table, do not include the extreme results of 0.75 from Cape

Mountain and the Atacama Desert, but use the upper and lower bounds separately, when ranges of values were given. The value 0.11 – 0.08 is 0.03, or 3% of the precipitation.

Table 2. Fog and/or dew contributions to annual mean precipitation, *P*.

Fraction of mean *P*	**Region**	**Reference**
0.75	Cape Mountain, S. Africa	Matimati (2009)
0.05 - 0.1	arid Andes valley	Kalthoff et al. (2006)
0.15	Balsa Blanca Spain (4-year mean)	Ucles et al. (2013)
0.19	semi-arid coastal south-western Madagascar	Hanisch et al. (2015)
0.27	sand dune areas of India (maximum)	Subramanian and Rao (1983)
0.049 - 0.102	continental semi-arid grassland	Aguirre-Gutierrez et al. (2019)
0.13	Chinese loess plateau	Yang et al. (2015)
0.111	Rambla Honda Spain	Moro et al. (2007)
0.1 - 0.25	Negev, Israel	Kidron (1999)
0.045	Netherlands grassland	Jacobs et al. (2006)
0.055 - 0.069	northern Germany	Xiao et al. (2009)
0.035 - 0.15	New Zealand snow tussock grasslands	Fahey et al. (2011)*
0.01 - 0.03	Upper Pilarcito Creek watershed, N. Calif.	Chung et al. (2017)
0.75	Atacama desert (0.8mm/yr = P)	Westbeld et al. (2009)
0.021 - 0.27	California coastal islands	Fischer et al. (2009)

* Note: Lower limit was within uncertainty of mean annual precipitation and upper limit was influenced by other factors, thus, both limits were possibly overestimations.

Significantly, only one of the above results, the Pilarcito Creek watershed of Chung et al. (2017), suggests a contribution to P of fog and dew that is as small as the up to 4% impact on the water balance from changes in storage. We therefore conclude that, although the statistical summary may be biased towards investigations of sites with particularly large contributions to P (that go unmeasured by traditional means), it is unlikely that the effect of fog and dew on ET is, on the average, smaller than that from changes in storage. Further, both effects are of the same sign and typically increase in a relative sense with increasing AI.

5. Discussion -- comparison with other models

A separate comparison with the data published by Duan et al. (2006) is warranted since it employs different variables, thus providing additional points of comparison. In the Duan et al. (2006) representations, the drawbacks of our model also show up more clearly in the emphasis of the sharpness of the distinction of the two results in their approach to AI = 1. In this comparison it should be kept in mind that sites that are, on the average energy-limited, may be water-limited for a significant portion of the year, and also vice-versa, meaning that a cross-over point in limiting quantities is actually spread out to a region of AI values. Our artificially sharp distinction is in need of improvement.

5.1. Comparisons with the Duan et al. (2006) data

The results of calculations using Eq. (11) for ET/PET are compared with the Budyko phenomenology using the Duan et al. (2006, Figure 3), and the data are shown in Figure 4. The data shown here were digitized from separate panels in their Figure 3 and compared with the Turc-Pike, Schreiber, and Oldekop formulations (Table 1).

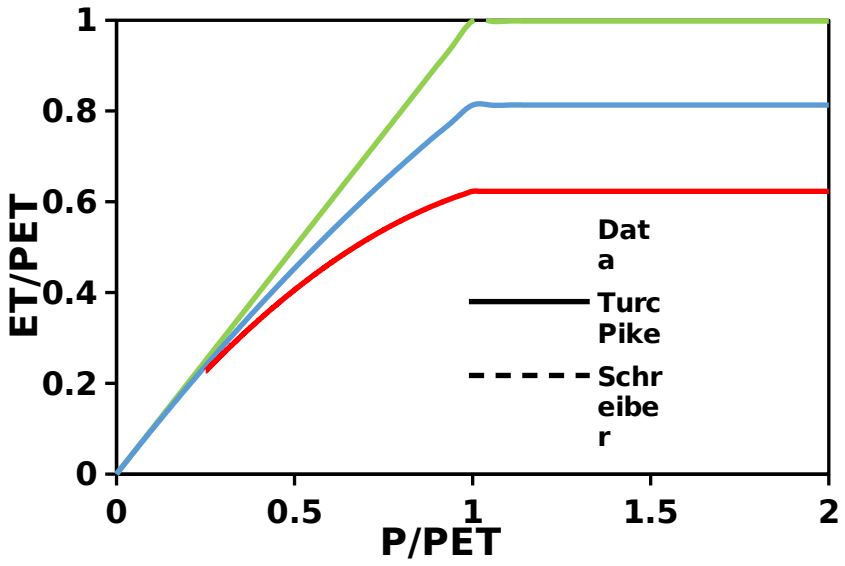

Figure 4. Comparison of the theoretical 2D and 3D predictions in the present theory (red and blue lines) with experimental Duan et al (2006) data (digitized from their Figure 3) and traditional phenomenological results. The maximum for ET/PET results when the plant root fractal dimensionality, $d_f = 3$. Whereas eight data points fall between the phenomenological predictions of Schreiber and Oldekop, 9 of the 12 data points fall between our theoretical predictions for 2D and 3D percolation values of the root fractal dimensionality.

We find that, despite the artificial appearance of the discontinuous change in slope, our theoretical predictions with $d_f = 1.9$ ($\alpha = 0.623$) and $d_f = 2.5$ ($\alpha = 0.813$) constrain the data slightly better than the Schreiber and Oldekop functions taken together. This conclusion would not change, if we used instead the values (2.65 and 1.79) given by Levang-Brilz and Biondini (2002) as describing the fractal dimensionalities of Grass 1 and Grass 2.

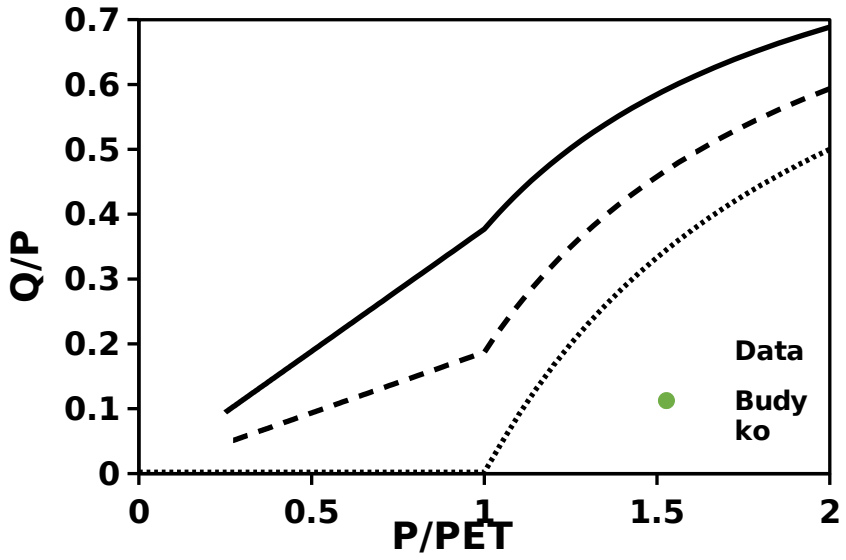

Figure 5. Predicted results for Q/*P* as a function of P/PET as compared with the Budyko phenomenology and data from Duan et al. (2006). As required from the results from Figure 4, nine of the 12 data points again fall between the 2D and 3D predictions.

Q/*P* from Eq. (9b) and Eq. (10b) is compared with existing phenomenologies using the Duan et al. (2006) data in Figure 5. A distinct discrepancy between our prediction and the phenomenology of Budyko is also noted at high values of PET, on account of the quadratic asymptotic form of the Budyko function (AI^{-2}). Here, at least, the data do not indicate that the predicted form is inferior to the Budyko phenomenology. But the question regarding the best choice for a theoretical expression in this limit is of significance to the more detailed comparison with the 50-year average Gentine et al. (2012) data set, which is an output of the MOPEX experiment and modeling described in Duan et al. (2006).

5.2. Comparison with data from Gentine et al. (2012)

In Figure 6, we compared predictions of ET/P as a function of PET/P with the annual ET data from Gentine et al. (2012). Since there was some indication in Figure 2 that theory underestimated experiment at high AI values, we

apply now in Figure 6 an adjustment to the data that is in general accord with overall studies on sea-level rise (Wada et al. 2017) and approximately tied to the specific hydrology of the western USA, as exemplified by the Columbia river, which shows that groundwater storage has been declining by as much as 4% of P annually (Liu et al. 2018). We use the 4% figure as a limit for the case AI → ∞ and apply a linear model based on the inverse of AI, with effects of storage change that vanish at AI = 1. The result thus predicts changes of only -1.5% for the Columbia River with its AI of 1.6, as well as -1.3% for the Mississippi and 0% for the Pearl River drainages, for which storage changes are -0.4% and -0.5%, respectively.

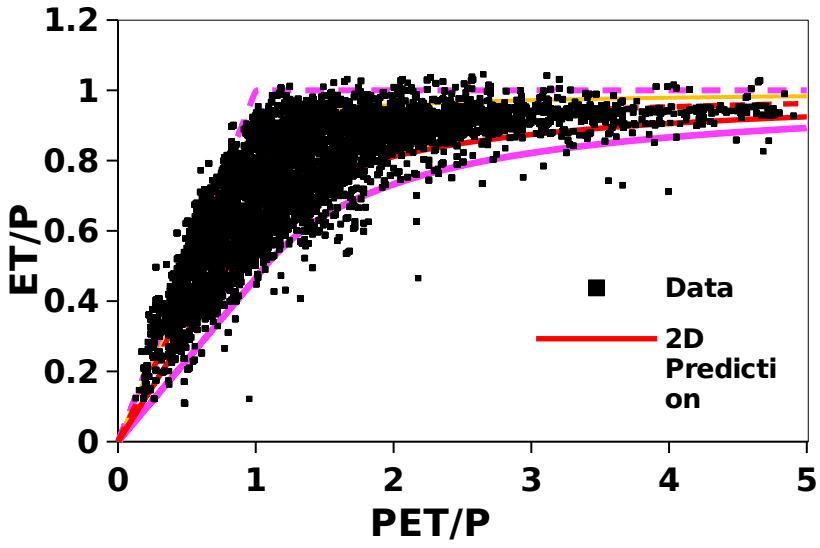

Figure 6. Comparison of the percolation predictions with data adjusted to reflect the tendency of groundwater storage to diminish in US stream basins, with an effect assumed linear in AI^{-1} between AI = 1 and AI = ∞. In this particular comparison, the maximum storage change in the limit of infinite AI is assumed to be 4%, approximately equal to the losses from the Columbia River (at AI = 1.64). The model thus underestimates storage losses in the Columbia and Pearl River basins, but overestimates such losses in the Mississippi basin. Note that such a correction places the large majority of the data points between the 2D and 3D percolation predictions at large AI, giving

the distribution a symmetric appearance with respect to theoretical predictions.

The comparison of the predictions of Eq. (8) and Eq. (10), using also the upper value of d_f from Grass 1 of Levang-Brilz and Biondini (2002) in Figure 6 allows several potentially important remarks. First is that the tendency to underestimate ET at high AI in Figure 2 can be removed by accounting for drawdown of groundwater storage. Second is that the lower limit of predicted ET values appears rather sharp, i.e., not plastic. Thus, values of ET below the lower limit are likely due to important characteristics that have been left out, such as the effects of snowmelt on the moisture content and groundwater recharge. The third is that, even when systematic trends in storage are removed, yearly summaries of ET/P still incorporate the effects of weather-related *fluctuations* in groundwater storage. However, in Figure 6, such fluctuations (typically under about 5%) appear equally spaced around the percolation predictions. In 26 large river basins globally (with overall mean ET/P ratio by area of 0.618), yearly fluctuations in storage appear to average about ± 3% (ET) (Liu et al., 2018). While subsurface storage changes can have either sign, positive or negative, in the USA and other regions with intensive agriculture, these changes are predominantly negative (Liu et al. 2018). Finally, at large AI, extreme desert conditions can restrict dominant vegetation types to a few species, such as, in the Mojave Desert, creosote bush (*Larrea tridentata*) and bursage (*Ambrosia dumosa*) (Hunt and Wu, 2004). With increasing aridity, the diversity of the ecosystem may suddenly change, if one of these species is unable to adapt. Evidence of this kind of discrete behavior may be present at AI > 3.5, where approximately horizontal rows of data, each terminating at a higher AI value, are present.

In Figure 7, the long-term (50-year average) results obtained by Gentine et al. (2012) are replotted and compared with predictions for $d_f = 1.9$ (2D), $d_f = 2.5$ (3D), and $d_f = 2.78$ (one standard deviation above the mean for Grass 1). In this representation, we also used the yearly average storage loss

(between 0% at AI = 1 and 4% in the limit AI →∞) as a fraction of P to reduce the ratio of ET/P generated from the models. As can be seen, for a wide range of AI, the data are found mostly between the 2D and 3D predictions, but the data tend to cross from an upper constraint of the 3D prediction to d_f = 2.78 at high AI. A sharp distinction between out-of-phase and in-phase data is noted, particularly at values of AI < 1, which will be addressed at a later date.

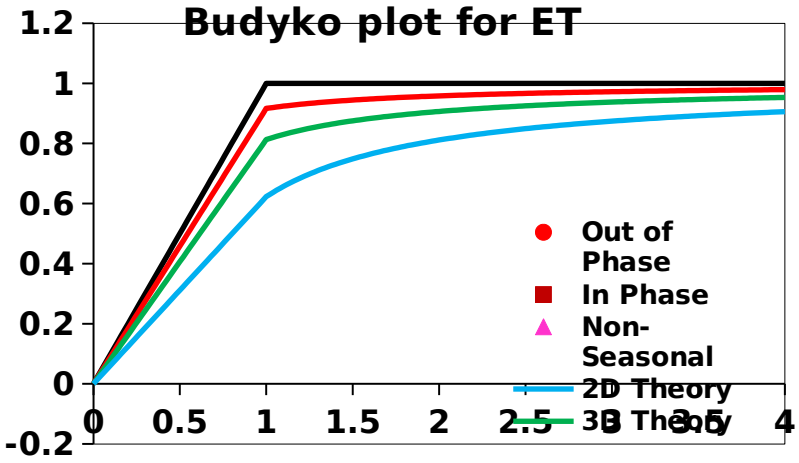

Figure 7. Comparison of Gentine et al. (2012) long-term ET data with 2D theory (d_f = 1.9), 3D theory (d_f = 2.5), the upper limit from the Gaussian model of observed Grass 1 d_f variability (“Gaussian High”), and the limit resulting from the maximum value of the root biomass fractal dimensionality of d_f = 3.

Particularly the in-phase data show a cross-over from constraints between 2D and 3D, to between 3D and ET = P as AI exceeds about 1.6. We address two possible reasons for this result: 1) under highly arid conditions, the dominant plant property of relevance is the ability to extract the maximum water possible (producing large d_f values), and 2) precipitation is underestimated for large AI.

While the 2D prediction (d_f = 1.9) provides a good lower bound for nearly all the data in Figure 7, the 3D prediction does not provide an upper bound, except for a relatively narrow range of AI between 1 and about 1.8. Nearly all the data falls above the 3D prediction for AL > 1.8. For AI < 1, the 3D value almost perfectly distinguishes between measurements of ET for in-phase and out-of-phase precipitation, with nearly all the in-phase values below 3D, and nearly all the out-of-phase results above it. Since these statistics involve hundreds of data points, the probability that this result is due to random variability is indistinguishable from zero. Our interpretation is that precipitation that arrives out of phase with the maximum in irradiance is not conducive to an optimal use of water by plants, but with increased water waste, here noted as evaporative losses. If this is correct, it is a result that is not in accord with current thinking (Berghuijs et al. 2014) regarding the role of seasonality of precipitation, though it is consistent in a more general sense with a recent study (Madany et al. 2021; discussed in Eos by Thompson, 2021) that showed a diminution of water use efficiency (WUE) when resources are scarce. In further support of this diagnosis, we find that non-seasonal drainages fall equally on both sides of the 3D prediction. We also note that typical phenomenologies in use would be unlikely to discover such a correlation, since they condense the variability in prediction curves dramatically in the low AI range relative to the large AI range, as noted in Figure 1.

In Figure 8, instead of using theoretical values of a plant-root fractal dimensionality, we use the actual, measured, values of d_f from Levang-Brilz and Biondini (2002) to predict ranges of ET. Grass 1 Max uses d_f = 2.78 as determined by the statistical methods described in section 4. We also show the prediction resulting from application of the maximum d_f value as found graphically (Grass 1 Max (alt)). As can be seen, now the lower and upper boundaries include nearly all of the data.

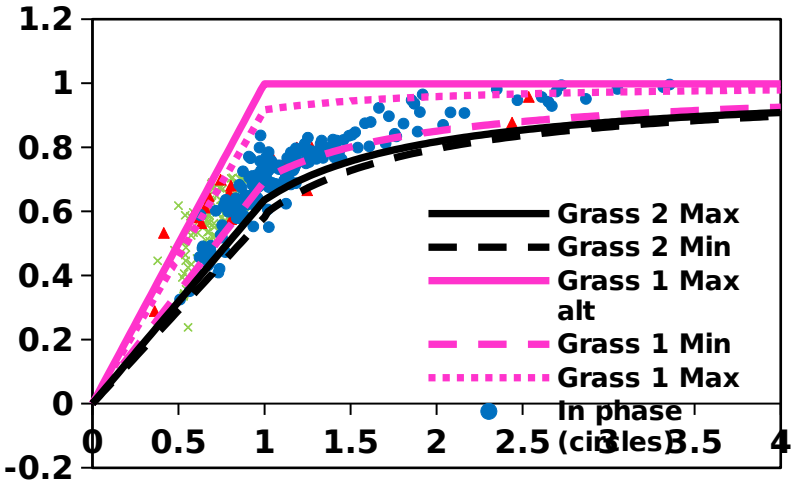

Figure 8. Comparison of theoretical ranges of ET predicted from the vegetation data for RLS as a function of BGM (below-ground biomass) as reported by Levang-Brilz and Biondini (2002). Grass 1 Max uses the d_f value found from the Gaussian approximation of the statistics of the variability of d_f, while Grass 1 Max (alt) determines a maximum d_f graphically (as described in section 4). In this figure, potential effects of storage changes are neglected. If neither storage losses nor precipitation underestimation is relevant, and if actual root fractal dimensionalities do not reach 3, then the present theory underestimates the large ET extreme for AI > 2.

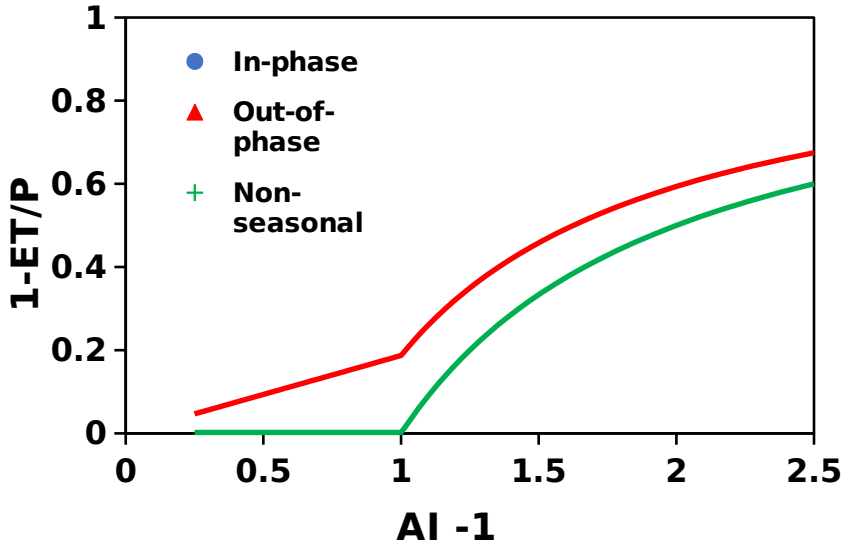

Figure 9. Comparison of the predictions of Eq. 9 and Eq. 10 with the full data set of Gentine et al. (2012). In the range $1 \leq AI^{-1} \leq 2$, it is noteworthy that nearly all the out of phase data fall between the 3D prediction and the $d_f = 3$ result, whereas nearly all the in-phase data fall between the 2D and 3D predictions. Also, the non-seasonal data are spread approximately evenly between the 2D prediction and $d_f = 3$ result. Note the discrepancy at low *P*/PET, which may be better represented by traditional phenomenology, e.g., Budyko (1958), which generates a quadratic dependence on 1/AI of 1 – ET/P. In Figure 10 this discrepancy is addressed.

Figure 9 uses the inverse of the aridity index and the variable 1 – ET/P (= Q/P) to clarify some relationships. This particular representation clarifies the distinction between in-phase and out of phase vegetation in the low AI regime. The general appearance of the data taken together could support a linear dependence of Q/P on the inverse aridity index, but which requires a threshold value of P/PET to be exceeded before run-off is measured. It could also support a quadratic dependence near 1/AI = 0, in line with the Budyko prediction. In Figure 10 below, we check whether alternative explanations could be relevant: 1) based on the hypothesis that underestimation of precipitation leads to an overestimation of the ratio ET/P, and 2) whether there is evidence that vegetation in arid environments adapts so that the fractal dimensionality of root system is increasing.

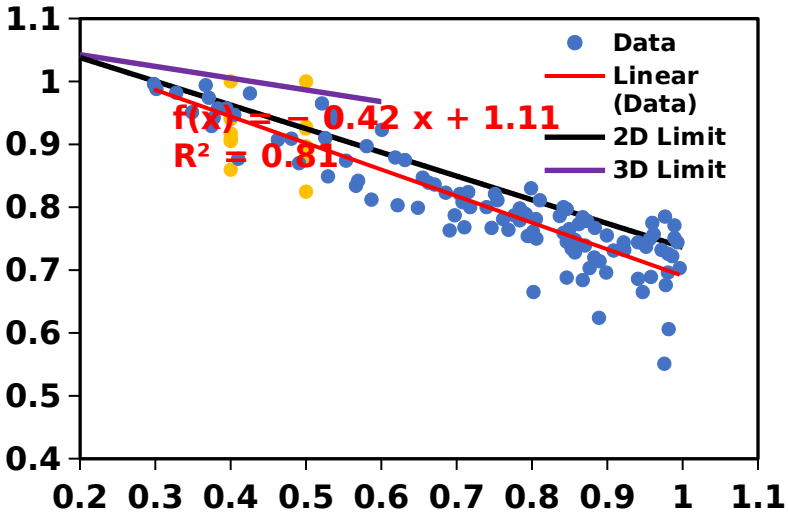

Figure 10. Plot of ET/*P* vs. *P*/PET for the Gentine et al. data set for AI ≥ 1.

The interpretation that underestimation of precipitation leads to the discrepancy between theory and prediction at large AI is supported in that the intercept (equal to extrapolated value of ET/P as AI approaches infinity) is equal to 1.11, which is a discrepancy equal to the mean underestimation of precipitation shown in Table 3. However, the selection of individual grasses from Grass Group 1 sweeps out the range of ET values shown, which cross over from the 2D limit to the 3D limit calculated using an 11% P underestimation assumption.

In Figure 10, we investigate the behavior of 1 – ET/P in the asymptotic limit of Ai → ∞. Grasses 0.5 and Grasses 0.4 refer to the predicted ET values at AI^{-1} = 0.5 and 0.4 of seven of the individual grass species identified as being in the group (Grasses 1) with aggregate fractal dimensionality of 2.65 (Levang-Brilz and Biondini, 2002). The reason for exclusion of 5 outlie values of d_f is that some of these values (such as d_f = 142, 5, and 1.5 for *Agropyron cristatum, Panicum virgatum*, and *Hordeum jubatum*) do not appear to be reasonable estimates for ecosystem d_f values. However, inclusion of these species in the determination of the standard deviation of the mean value of *s*

= 1/ d_f does not change the statistics substantially. Overall, we find support for any of the possible interpretations mentioned. While a systematic error of 11% in precipitation may seem large, it should be noted that nearly 4% of P annual drawdown of storage is documented in Liu et al. (2018) already for the Columbia River, with basin average AI of 1.64 (in this area, a climate designated as semi-arid). Thus, even a significant exaggeration of the underestimation of precipitation is at least partially compensated by a lack of simultaneous accounting for systematic changes in storage.

6. Summary and Conclusions

The advantage of our treatment lies less in how it constrains the data overall, but in the specific diagnostics from: 1) distinct regions of AI, and 2) distinct results from different types of ecosystems. For example, vegetation that receives precipitation in phase with the maximum in solar irradiance seems, for AI near or below 1 to have significantly higher water use efficiency than out-of-phase vegetation, while at higher AI values, this situation may well be exactly reversed. As for resolving the discrepancy between the percolation prediction and the Budyko prediction at high AI values, in-phase vegetation seems to favor more the Budyko hypothesis (a power very near 2, as predicted), whereas out-of-phase and non-seasonal vegetation generate a power near 1 or, when a linear function is fitted, an intercept near zero and a high correlation coefficient (none of these results are shown).

The variability of d_f among grass species predicts a greater variability of ET than is observed, once impacts from changes in yearly storage are removed by taking long-term averages. It is not likely that this result implies the lack of relevance of other variables. However, It does appear to imply that the single variable, d_f of the root system, is the dominant influence in determining the variability of ET at any particular value of the aridity index.

Finally, the apparent relevance of only the 2D exponent to the global response suggests that, at very large scales (continental to global), the relevance of local variations in PET/P is smoothed out, while the critical zone and its productivity are effectively constrained to such a narrow depth that it behaves overall like a 2D system. This trend of a reduction in ET with scale is, in general, also consistent with reported results of Choudhury (1999), in which ET for drainage basins was smaller, on average, than for specific stations.

Although Budyko (1958, 1974) yields results that are often in accord with data, the spread in experimental values for ET/P at any particular PET/P has invited generalizations to incorporate adjustable parameters. A physically-based optimization of ecosystem net primary productivity, NPP, with respect to the primary hydrologic fluxes, ET (evapotranspiration) and Q (run-off, including subsurface flow) has been incorporated into a theory of the water balance broadly compatible with the Budyko formulation. The optimization is based on a competition for soil water resources between soil depth input and lateral root development. The results yield the fraction of precipitation returned to the atmosphere as ET as a function of the aridity index AI = PET/P. Variability in ET at each particular value of AI is determined by a parameter that combines exponents d_f and D_b (corresponding to plant root fractal dimensionality and the fractal dimensionality of the percolation backbone) of percolation scaling relationships for vegetation growth and soil development. In accord with a wide range of studies on soil formation and landscape evolution, D_b is assumed universal (and equal to 1.87), as predicted by percolation theory. Much more limited plant root data agree approximately with the predictions from percolation theory (1.9 for highly anisotropic, mainly lateral development, 2.5 for isotropic development), in that reported values for $1/d_f$ from a study of 55 species that populate the Great Plains ecosystem are characterized by the following three values, 1.79, 2.5, and 2.65, which are rather close to percolation predictions of 1.9 (2D)

and 2.5 (3D). Qualitatively, the extreme values allowed in the parameters as defined by individual 2D and 3D plant root fractal dimensionalities sweep out a somewhat wider range of ET/*P* values as a function of aridity index than do either traditional phenomenologies or the percolation theoretical values. Theoretical limiting values of $d_f = 1$ and 3 produce relatively accurate limits on the annual ET data. Theoretical predictions overall seem to generate poorer agreement with 50-year average experimental values under water-limited conditions than under energy-limited conditions. At high aridity index, our predictions mostly underestimate the upper limit of ET values. Though our theoretical description is distinct from Budyko's in this range, the Budyko prediction is also an underestimation. Investigations of mean annual ET values reveal a similar underprediction of ET at large AI values, though the discrepancy is of smaller magnitude and appears likely to be due to mining groundwater in the western USA.

More detailed investigations of the 50-year average dry-end behavior of ET/*P* as a function of PET/*P* do not conclusively distinguish between the choices of a functional representation of ET/P, nor do they allow clear conclusions regarding a physical mechanisms that could confound the data (systematic storage changes, precipitation underestimation, sometimes referred to as undercatch), or its interpretation (possible threshold P value for run-off, superiority of a different phenomenology, change in vegetation characteristics with aridity). The magnitude of that inferred underestimation (11% in the limit of extreme aridity) appears to be in agreement with a summary of the existing literature, documenting a typically overlooked ca. 11% contribution to arid region *P* from such causes as dew and fog. Whether this is the cause of our underestimation of ET is not clear, since our summary of published data may represent a bias towards regions with significant effects. An alternative, more ecologically- or geomorphologically-based hypothesis should also be considered, however. In arid environments, either diffusion of raindrop-eroded soil to plants (Planchon and Mouche, 2010) or

accumulation of aeolian sediments under plants (Field et al. 2010) might mitigate against the need for plants to allow water infiltration for soil development, thus decoupling the processes of soil genesis and plant growth, together with their associated hydrologic fluxes. Then it would be possible that the maximum NPP value occurs at an endpoint (ET/P = 1) of the ET/P domain, rather than at a local maximum. Such a maximum cannot be found by setting a derivative equal to zero, since maximum NPP is, in that case, generated from the maximum possible transpiration. In our model, this would be accomplished by suitable root development (any value of $d_f \geq 3$), which allows all water to be withdrawn from the subsurface. Such a change in mechanism might occur rather abruptly with increasing AI values.

It may be important that, contrary to our initial expectation (Hunt 2021; Hunt et al. 2020ab), the 3D prediction does not provide a good upper bound for deduced watershed ET/P values as a function of AI. It represents more nearly a typical value for ET/P. Similarly, instead of representing a typical value of ET/P, the 2D prediction conforms much more closely to a lower bound of watershed ET/P. Nevertheless, it is the 2D value of the percolation fractal dimensionality, 1.9, which, when applied to energy and water neutral conditions (AI = 1), yields $ET = 0.623\ P$, which only diverges from the global average by about 1.5%. While this may have a simple explanation from statistical averaging over AI values, particularly if NPP magnitudes are higher in energy-limited ecosystems (for which ET is a smaller fraction of P) than in water-limited cases, for example, we speculate that it may actually have a physical, rather than purely statistical, explanation. On planetary scales, it may be reasonable to assume, in the mean, the relevance of neither water nor energy limitations to continental ecosystems. Also, on the scale of a continent (10^7m), the root zone (ca. 1m) is exceedingly shallow. Thus, the assumptions that energy/water limitations can be neglected and that the percolation cluster fractal dimensionality in 2D can be considered an

appropriate description for a terrestrial ecology, may be much better justified in the global aggregate than for individual watersheds.

Additionally, we wish to identify a lower bound for ET/P, consistent with the hypotheses here. Particularly for a lower-limit on ET, snow-dominated catchments must be excluded on account of the significance of the input of solar energy to melting. Indeed, the opposite shift from snow dominated to rain dominated catchments has been shown to increase ET (Berghuijs et al. 2014). And, in a related study, Zhang et al. (2015) demonstrated that virtually all of the anomalously low ET values for AI greater than about 2 were associated with catchments with more than 10% of the precipitation arriving as snow.

Clearly, it would be advantageous for predictive capabilities to develop a smoother cross-over linking the predictions for AI < 1 and AI > 1. Our treatment generates such a cross-over through its assumption of watershed level conditions that are uniformly either energy-limited or water-limited. Such an advance in theoretical capabilities can probably be developed through a statistical approach that is based on information as to how often conditions in drainages with AI > 1 are actually energy-, rather than water-limited, and vice-versa. It remains a goal for future work.

Acknowledgment

BG is grateful to Kansas State University for support through faculty startup funds. BF research was partially supported by the SFA Watershed and Deduce projects, funded by the U.S. DOE, Office of Science, Office of Biological and Environmental Research, and Office of Advanced Scientific Computing under contract DE-AC02-05CH11231.

References

Aguirre-Gutiérrez, C. A., Holwerda, F., Goldsmith, G. R., Yepes, E., Carbajal, N., Escoto-Rodríguez, M., and Arredondo, J. T., 2019, The importance of

dew in the water balance of a continental semi-arid grassland, 2019, J. Arid Environments 168; 26-35.

Barker, W.T.; Whitman, W.C. Vegetation of the northern Great Plains. Rangelands 1988, 10, 266–272.

Berghuijs, W. R., Woods, R, and Hrachowitz, M., 2014. A precipitation shift from snow towards rain leads to a decrease in streamflow, Nat. Clim. Chang. 4: 583-586. 10.1038/NCLIMATE2246

Berghuijs, W., Gnann, S. J., and Woods, R. A., 2020. Unanswered questions on the Budyko framework, Hydrological Processes. 34: 5699–5703

Budyko, M.I. The Heat Balance of the Earth’s Surface; Translated 1958 by N. A. Stepanova; US Dept. of Commerce, Weather Bureau: Washington, DC, USA, 1956.

Budyko, M.I. Climate and Life; Academic: San Diego, CA, USA, 1974; 508p.

Bundt, M., Widmer, F., Pesaro, M., Zeyer, J., and Blaser, P., 2001. Preferential flow paths: biological ’hot spots‘ in soils, Soil Biology and Biogeochemistry, 33 (6) 729-738.

Chen, H., Huo, Z., Zhang, L., and White, I., 2020. New perspective about application of extended Budyko formula in arid irrigation district with shallow groundwater, J. Hydrol. 582: 124496.

Choudhury, B. J.: Evaluation of an empirical equation for annual evaporation using field observations and results from a bio-physical model, J. Hydrol., 216, 99–110, doi:10.1016/s0022-1694(98)00293-5, 1999

Chung, M. Dufour, A., Pluche, R., and Thompson, S., 2017, How much does dry-season fog matter? Quantifying fog contributions to water balance in a coastal California watershed, Hydrologic Processes 31: 3948-3961.

Dai, A.; Trenberth, K.E. 2002. Estimates of freshwater discharge from continents: Latitudinal and seasonal variations. J. Hydrometeorol., 3, 660–687, doi:10.1175/1525-7541003<0660:EOFDF.

Dai, A.; Qian, T.T.; Trenberth, K.E.; Milliman, J.D. 2009. Changes in continental freshwater discharge from 1948 to 2004. J. Clim., 22, 2773–2792, doi:10.1175/2008JCLI2592.1.

Duan, Q., et al. (2006), Model Parameter Estimation Experiment (MOPEX): An overview of science strategy and major results from the second and third workshops, J. Hydrol.,320,3–17, doi:10.1016/j.jhydrol.2005.07.031

Eagleson, P.S. Climate, soil, and vegetation: 1. Introduction to water balance dynamics. Water Resour. Res. 1978a, 14, 705–712, doi:10.1029/WR014i005p00705.

Eagleson, P.S. Climate, soil, and vegetation: 2. The distribution of annual precipitation derived from observed storm sequences. Water Resour. Res. 1978b, 14, 713–721.

Eagleson, P.; Tellers, T. Ecological optimality in water-limited natural soil-vegetation systems: 2. Tests and applications. Water Resour. Res. 1982, 18, 341–354, doi:10.1029/WR018i002p00341.

Egli, M.; Hunt, A.G.; Dahms, D.; Raab, G.; Derungs, C.; Raimondi, S.; Yu, F. Prediction of soil formation as a function of age using the percolation theory approach. Front. Environ. Sci. 2018, 28, doi:10.3389/fenvs.2018.00108.

Field, J. P, Belnap, J., Breshears, D. D., Neff, J. C., Okin, G. S., Whicker, J. J., Painter, T. H., Ravi, S., Reheis, M. C., and Reynolds, R. L., 2010. The ecology of dust, Front. Ecol. Environ. 8(9): 423-430.

Fischer, D. T., Stillz, C. J. and Williams, A. P., 2009. Significance of summer fog and overcast for drought stress and ecological functioning of coastal California endemic plant species, Journal of Biogeography, 3:, 783–799.

Fahey, B., Davie, T. and Stewart. M., 2011. The application of a water balance model to assess the role of fog in water yields from catchments in the east Otago uplands, South Island, New Zealand, Journal of Hydrology (NZ) 50 (2): 279-292.

Fan, Y.; Miguez-Macho, G.; Jobbágy, E.G.; Jackson, R.B.; Otero-Casal, C. Hydrologic regulation of plant rooting depth. Proc. Natl. Acad. Sci. USA 2017, 114, doi/10.1073/pnas.1712381114.

Flury, M., and Flühler, H., 1994. Susceptibility of soils to preferential flow of water: a field study, Water Resources Research, 30: 1945-1954.

Fu, B.: On the calculation of the evaporation from land surface, Scientia Atmospherica Sinica, 5, 23–31, 1981 (in Chinese)

Gentine, P.; D'Dodorico, P.; Linter, B.R.; Sivandran, G.; Salvucci, G.; Interdependence of climate, soil, and vegetation as constrained by the Budyko curve. Geophys. Res. Lett. 2012, 39, L19404, doi:10.1029/2012GL053492.

Guswa, A. 2008. The influence of climate on root depth: A carbon cost-benefit analysis. Water Resour. Res. 44, W02427.

Guswa, A. 2010. Effect of plant uptake strategy on the water—Optimal root depth. Water Resour. Res. 46, W09601. 56.

Hanisch, S., Lohrey, C., Buerkert, A. 2015. Dewfall and its ecological significance in semi-arid coastal south-western Madagascar, J. of Arid Environments 121: 24-31

Hunt, A. G., and Wu, J. 2004. Climatic influences on Holocene variations of soil erosion rates on a small hill in the Mojave Desert, Geomorphology 58: 263-289.

Hunt, A.G. Spatio-temporal scaling of vegetation growth and soil formation: Explicit predictions. Vadose Zone J. 2017, doi:10.2136/vzj2016.06.0055

Hunt, A. G., 2020, Soil formation, vegetation growth, and water balance: A theory for Budyko, in Hunt, A. G., Egli, M. and Faybishenko, B. A., Hydrogeology, Chemical Weathering, and Soil Formation, Geophysical Monographs, AGU.

Hunt, A. G., and Manzoni, S., 2015, Networks on Networks: The Physics of Geobiology and Geochemistry, IOP Publishing, UK.

Hunt, A. G., and B. Ghanbarian, 2016, Percolation theory for solute transport in porous media: Geochemistry, geomorphology, and carbon cycling, *Water Resources Research*, 52: 7444-7459

Hunt, A. G., Holtzman, R., Ghanbarian, B., 2017. A percolation-based approach to scaling infiltration and evapotranspiration, Water, 9(2): 104-https://doi.org/10.3390/w9020104

Hunt, A. G., Faybishenko, B. A., Egli, M., Ghanbarian, B., and Yu, F. 2020a, Predicting water cycle characteristics from percolation theory and observational data, Int. Journ. Env. Res. & Pub. Health. 17: 734-751.

Hunt, A. G., Faybishenko, B. A., and Ghanbarian, B., 2020b, Predicting the water balance from optimization of plant productivity, GSA Today, 30 https://doi.org/10.1130/GSATG71GW.1.

Hunt, A. G. Faybishenko, B. A., and Powell, T. L. 2020c A new phenomenological model to describe root-soil interactions based on percolation theory, Ecological Modelling 433: 109205.

Jacobs A. F. G., Heusinkveld B. G., Wichink Kruit R. J., Berkowicz S. M. 2006. Contribution of dew to the water budget of a grassland area in the Netherlands. Water Resources Res 42: W03415. doi:10.1029/2005WR004055

Jasechko, S. Global isotope hydrogeology. Rev. Geophys. 2019, 57, 835–965. 10.1029/2018RG000627.

Kalthoff, N., Fiebig-Wittmaack, Meissner, C., Kohler, M., Uriarte, M., Bischoff-Gauss, I., and Gonzales, E., 2006, The energy balance, evapo-transpiration, and nocturnal dew deposition of an arid valley in the Andes, Journal of Arid Environments 65(3) 420-443

Khormali, F., Ghergherechi, S., Kehl, M., and Ayoubi, S., 2012. Soil formation in loess derived soils along a sub-humid to humid climate gradient, northeast Iran, Geoderma 179-180: 113-122.

Kidron, G. 1999. Altitude dependent dew and fog in the Negev Desert, Israel, Agricultural and Forest Meteorology, 96 (1-3) 1-8.

Lee, Y, J.S. Andrade, S.V. Buldyrev, N.V. Dokholoyan, S. Havlin, P.R. King, G. Paul, and H.E. Stanley, 1999, Traveling time and traveling length in critical percolation clusters, *Phys. Rev. E* **60** (3): 3425–3428.

Levang-Brilz, N.; Biondini, M.E. 2002. Growth rate, root development and nutrient uptake of 55 plant species from the Great Plains Grasslands, USA. Plant Ecol., 165, 117–144.

Liu, J., Zhang, Q., Singh, V. P., Song, C., Zhang, Y., Sun, P., and Gu, X., 2018. Hydrological effects of climate variability and vegetation dynamics on annual fluvial water balance in global large river basins, Hydrol. Earth Syst. Sci., 22, 4047–4060, https://doi.org/10.5194/hess-22-4047-2018

Liu, Y. Wagener, T., Beck, H. E., and Hartman, A., 2020. What is the hydrologically effective area of a catchment, Environmental Research Lettes 15: 104024 https://doi.org/10.1088/1748-9326/aba7e5

Lvovitch, M.I. 1973. The global water balance: U.S. National Committee for the International Hydrological Decade. U.S. Natl. Comm. Int. Hydrol. Decade Bull., 23, 28–42, doi:10.1029/EO054i001p00028.

Lynch, J. 1995. Root architecture and plant productivity. Plant Physiol., 109, 7–13.

Madany, T. S., Reichstein, M., Carrara, A., Martin, M. P., Gonzales-Cascon, R., Penuelas, J., Ellsworth, D. S., Burcard-Levine, V., Hammer, T. W., Knauer, Juergen, Kolle, O., Luo, Y., Pacheco-Labrador, J., Nelson, J. A., Perez-Priego, O., Roto, V., Wutler, T., and Migliavacca, M., 2021. How nitrogen and phosphorus availability change water use efficiency in a Mediterranean savannah ecosystem, JGR Biogeosciences, 126: https://doi.org/10.1029/2020JG006005

Manabe, S. Climate and ocean circulation. I. Atmospheric circulation and hydrology of the Earth's surface. Mon. Weather Rev. 1969, 97, 739–774, doi:10.1175/1520-04930972.3.CO;

Matimati, I., 2009, The relevance of fog and dew precipitation to succulent plant hydrology in an arid South African ecosystem, Master's Thesis, University of the Western Cape, S. Africa

Milne, B.; Gupta, V. 2017. Horton ratios link self-similarity with maximum entropy of eco-geomorphological properties in stream networks. Entropy, 19, 249, doi:10.3390/e19060249.

Moratiel, R., Martínez-Cob, A., Tarquis, A. M, and Snyder, R. L., 2016. Water balance correction due to light rainfall, dew, and fog in Ebro river basin (Spain), Agricultural Water Management, 170: 61-67

Moro, M. J., Were, A., Villagarcia, L., Canton, Y., Domingo, F., 2007, Dew measurement by Eddy covariance and wetness sensor in a semiarid ecosystem of SE Spain, Journal of Hydrology, 335 (304): 295-302.

National Research Council,.1996. Rock fractures and fluid flow. Washington, DC: National Academy Press.

Oki, T.; Kanae, S. Global hydrological cycles and world water resources. Science 2006, 313, 1068–1072, doi:10.1126/science.1128845.

Oldekop, E. M. (1911), On evaporation from the surface of river basins, *Trans. Meteorol. Obs. Univ. Tartu, 4, 200.*

Pike, J. G. (1964), The estimation of annual run-off from meteorological data in a tropical climate, J. Hydrol.,2(2), 116–123, doi:10.1016/0022-1694(64)90022-8.

Planchon, O., and Mouche, E., 2010. A physical model for the action of raindrop erosion on soil microtopography, Soil Sci. Soc. Amer. J. 74: 1092-1103 https://doi.org/10.2136/sssaj2009.0063

Porto, M.; Havlin, S.; Schwarzer, S.; Bunde, A. Optimal path in strong disorder and shortest path in invasion percolation with trapping. Phys. Rev. Lett. 1997, 79, 4060–4062.

Potter, N. J., L. Zhang, P. C. D. Milly, T. A. McMahon, and A. J. Jakeman (2005), Effects of rainfall seasonality and soil moisture capacity on mean annual water balance for Australian catchments, *Water Resour. Res.*, 41, W06007, doi:10.1029/2004WR003697.

Rodriguez-Iturbe, I.; Porporato, A.; Ridolfi, L.; Isham, V.; Cox, D.R. 1999. Probabilistic modelling of water balance at a point: The role of climate, soil and vegetation. Proc. R. Soc. Lond. A 455, 3789–3805.

Sahimi, M. 1994. Applications of Percolation Theory, Taylor & Francis, London.

Schlesinger, W.H.; Jasechko, S. Transpiration in the global water cycle. Agric. For. Meteorol. 2014, 189, 115– 117, doi:10.1016/j.agrformet.2014.01.011.

Schreiber, P. (1904), Ueber die Beziehungen zwischen dem Niederschlag und der Wasserfuehrung der fluesse in Mitteleuropa*, Meteorol. Z., 21, 441–452.*

Sheppard, A.P., M.A. Knackstedt, W.V. Pinczewski, and M. Sahimi, 1999, Invasion percolation: new algorithms and universality classes, *J. Phys. A: Math. Gen*. **32**: L521–L529.

Sposito, G. (2017a), Understanding the Budyko equation. *Water* 2017, 9.

Sposito, G. (2017b), ***Incorporating the Vadose Zone into the Budyko Framework,*** *Water* **2017**, *9*(9), 698.

Stagnitti, F., Parlange, J.-Y. Steenhuis, T. S., Boll, J. Pivetz, B., Barry, D. A. 1995: In, Transport of moisture and solutes in the unsaturated zone by preferential flow V.P. Singh (Ed.), Environmental Hydrology, Kluwer Academic Publishers, Dordrecht (1995), 193-224.

Subramanian, A. R., and Rao, A.V.R.K, 1983, Dewfall in sand dune areas of India, International Journal of Biometry, 27: 271-280

Thompson, E. 2021. A well-balanced ecosystem uses water most efficiently, *Eos, 102,* https://doi.org/10.1029/2021EO158043. Published on 13 May 2021.

Uclés, O., Villagarcía, L., Moro, M. J., Canton, Y., and Domingo, F. 2014. Role of dewfall in the water balance of a semiarid coastal steppe ecosystem, Hydrol. Process.28, 2271–2280.

Wada, Y., Reagers-Benjamin, J. T., Chao, F., Wang, J., Lo, M.-H., Song, C., Li, Y., and Gardners, A. S., 2017. Recent changes in land water storage and its contribution to sea level variations, Surv. Geoph. 38: 131-152.

Wang, D.; Wang, G.; Anagnostou, E.N. Evaluation of canopy interception schemes in land surface models. J. Hydrol. 2007, 347, 308–318.

Westbeld, A., Klemm, O., Grießbaum, F., Sträter, E., Larrain, H., Osses, P., and Cereceda, P., 2009. Fog deposition to a Tillandsia carpet in the Atacama Desert, Ann. Geophys., 27, 3571–3576, 2009.

Williams, C.A.; Reichstein, M.; Buchmann, N.; Baldocchi, D.; Beer, C.; Schwalm, C.; Wohlfahrt, G.; Hasler, N.; Bernhofer, C.; Foken, T.; et al. Climate and vegetation controls on the surface water balance: Synthesis of evapotranspiration measured across a global network of flux towers. Water Resour. Res. 2012, 48, W06523, doi:10.1029/2011WR011586.

Xiao, H., Meissner, R., Seeger, J. Rupp, H. and Borg, H., J. 2009. Effect of vegetation type and growth stage on dewfall determined with high precision weighing lysimeters at a site in northern Germany, Hydrology 377: 43-49.

Yang, H., Yang, D., Lei, Z., and Sun, F.: New analytical derivation of the mean annual water-energy balance equation, Water Resour. Res., 44, W03410, doi:10.1029/2007wr006135, 2008.

Yang, F.-L., Yue, P., Yao, T., and Wang, W.-Y, 2015. Characteristics of dew formation and distribution and its contribution to the surface water budget in a semi-arid region in China. Boundary Layer Meteorology, 154:317-331.

Yu, F., and Hunt, A. G., 2017a, Predicting soil formation on the basis of transport-limited chemical weathering, *Geomorphology*, https://doi.org/10.1016/j.geomorph.2017.10.027.

Yu, F., and Hunt, A. G. 2017b. An examination of the steady-state assumption in soil development models with application to landscape evolution. Earth Surface Processes and Landforms, 42(15), 2599–2610. https://doi.org/10.1002/esp.4209.

Yu, F. and A. G. Hunt, 2017c, Damköhler number input to transport-limited chemical weathering and soil production calculations, Earth and Space Chemistry. DOI: 10.1021/acsearthspacechem.6b00007

Yu, F., B. Faybishenko, A. G. Hunt, and B. Ghanbarian, 2017, A simple model of the variability of topsoil depths *Water* 9 (7) 460 doi:10.3390/w9070460

Yu, F., A. G. Hunt, M. Egli, and G. Raab, 2019, Comparison and contrast in soil depth evolution for steady-state and stochastic erosion processes: Possible implications for landslide prediction, *Geochemistry, Geophysics, Geosystems*, https://doi.org/10.1029/2018GC008125.

Zhang, L., Dawes, W. R., and Walker, G. R., 2001. Response of mean annual evapotranspiration to vegetation changes at catchment scale, Water Resourced Research 37 701-708.

Zhang, L., Hickel, K., Dawes, W. R., Chiew, F. H. S., Western, A. W., and Briggs, P. R., 2004. A rational function approach for estimating mean annual evapotranspiration, Water Resour. Res. 40: W02502 14pp. https://doi.org/10.1029/2003WR002710

Zhang, L., N. Potter, K. Hickel, Y. Zhang, and Q. Shao (2008), Water balance modeling over variable time scales based on the Budyko framework—Model development and testing, *J. Hydrol.*, 360, 117– 131, doi:10.1016/j.jhydrol.2008.07.021.

Zhang, D., Cong, Z., Ni, G., Yang, D., and Hu, S. 2015. Effects of snow ratio on annual run-off within the Budyko framework, Hydrology and Earth Systems Science 19: 1977-1992 www.hydrol-earth-syst-sci.net/19/1977/2015/doi:10.5194/hess-19-1977-2015.